

# Bound states of charges on top of graphene in magnetic field

Sergey Slizovskiy\*

Department of Physics, Loughborough University,  
Loughborough LE11 3TU, UK and  
NRC “Kurchatov Institute” PNPI, Russia

Charges put on top of graphene can move at elevated temperatures or if these charges are the intrinsic electron or hole states in the surface band of substrate such as SiC. We show that in the external magnetic field like charges on top of graphene may be mutually attracted to form macro-molecules. The size of the resulting macro-molecules is of the order of the magnetic length. Tuning the doping of graphene or the magnetic field, the binding of impurities can be turned on and off and the macro-molecule size may be tuned. We classify all the possible stable macro-molecules that unit charges can form on graphene in magnetic field. We argue that the binding survives the high temperatures. This opens the perspective to nanoscopic manipulation of ions on graphene by using macroscopic tools.

PACS numbers: 75.70.Ak , 73.22.Pr, 12.20.Ds

## I. INTRODUCTION

Ten years since discovery of graphene<sup>1</sup>, and it's applications range from cancer-drug delivery<sup>2,3</sup> to novel electronic devices. Still, many of proposed uses of graphene depend crucially on it's interface interactions with other compounds and impurities. In this sense, one could think of different graphene types with subtle, but important differences in the properties. Typically, molecular dynamics and DFT methods are used to model the interaction of graphene with substrate and impurities, while the 2D field theory is used to model the intrinsic electronic properties of graphene.

In this work we discuss the interaction between charged impurities on the surface of graphene and show that graphene in magnetic field can produce either attraction or repulsion of charged impurities, depending on the strength of the magnetic field and doping. We show that impurity ions on top of graphene can under certain conditions bind into macro-molecules with the size of the molecule of the order of the magnetic length (around 10 nm for magnetic field  $B \approx 10T$ ). Graphene in magnetic field serves as an excellent conductor for the electron hybridization cloud that can lead to attraction exceeding the Coulomb repulsion of same-charge ions, see fig.1. Similarly to the signatures of Quantum Hall Effect (QHE)<sup>4</sup>, we show that the effect survives the room temperature.

It is traditional to consider static impurities in the context of electronic systems in magnetic field (Quantum Hall effect). Here we break this tradition and consider impurities that can change location. The original motivation for this comes from epitaxial graphene on C-terminated SiC<sup>5-8</sup>, where positively-charged donors appear dynamically in the “dead” layer just below graphene<sup>9-11</sup>. This process looks as the appearance of localized hole in the insulating “dead” layer and an electron “dissolving” in graphene. Apart from the example of epitaxial

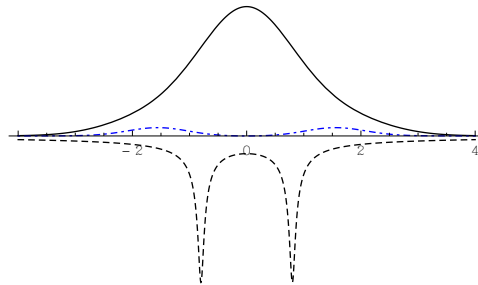


FIG. 1. Illustration of A and B sublattice wavefunctions  $|\psi_A|^2$ ,  $|\psi_B|^2$  for the lowest-energy sublevel of 0-th LL; and Coulomb potential of two charges (dashed).

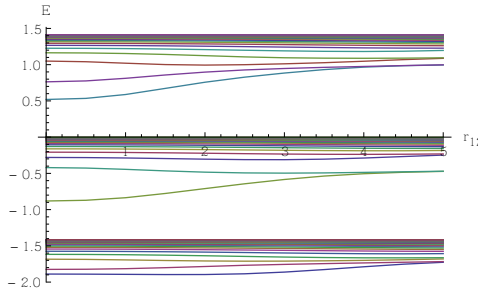


FIG. 2. Illustration of energy sub-levels for three Landau levels as a function of distance between two positively charged Coulomb centers. Here  $\alpha = 0.4$  and  $d = 0.05$ .

graphene, one could imagine any mobile ion near graphene or any molecule (even peptide<sup>2,3</sup>) donating electron to graphene or accepting it. For definiteness, we consider positively charged ions below, but exactly the same description applies to the negative ions if one makes a particle-hole transformation and reverts the sign of chemical potential.

Without magnetic field, graphene will produce non-linear screening of external charges<sup>12,13</sup>. When magnetic field is applied, the ordinary screening is significantly suppressed<sup>14,15</sup> and electrons become localized. The magnetic localization length (mag-

netic length  $l_B = \sqrt{\hbar/(eB)}$ ) is typically much larger than the atomic scales and when several charged impurities are at the distance of order of  $l_B$ , they can form stable molecules bound by the electrons in graphene. As will be explained below, graphene is capable of binding either positive or negative ions, depending on its filling fraction. In other words, the effect may be called *over-screening of Coulomb repulsion* of impurities.

Our results are summarized in the phase diagram table I. We suggest that this effect could be used in the controlled deposition and patterning of impurities, and as a basis for microscopic studies of Quantum Hall effect in graphene with non-rigid impurities.

TABLE I. Phase diagram for positively charged ions at  $\alpha = 0.4$ ,  $d = 0.05l_B$ ; for negatively-charged ions one has to replace  $\mu \rightarrow -\mu$

lowest $\mu$	positive ion configuration	bound electrons
-0.93	3 in triangle, $r_{ij} \approx 1.5l_B$	2 in symmetric state
-0.75	2, $r_{12} \approx 1.7l_B$	1
-0.63	2, $r_{12} \approx 1.3l_B$	2 in symmetric state
-0.45	1	1
-0.28	1	2 in symmetric state
0.51	3 in triangle, $r_{ij} \approx 1.4l_B$	2 in symmetric state
0.67	2, $r_{12} \approx 1.5l_B$	1
0.82	2, $r_{12} \approx 1.2l_B$	2 in symmetric state
1.02	1	1
1.19	1	2 in symmetric state

## II. GRAPHENE WITH CHARGED IMPURITIES IN MAGNETIC FIELD

It is well-known that the one-particle energy levels of an ideal graphene in magnetic field  $B$  are given by degenerate Landau levels<sup>1,16-18</sup>:

$$E_n = \text{sign}(n)E_B\sqrt{2|n|}, n \in \mathbb{Z} \quad (1)$$

where  $v_F \approx 10^6 \text{ m/s}$ ,

$$l_B = \sqrt{\hbar/(eB)} \approx 26 \text{ nm} / \sqrt{B/(\text{Tesla})} \quad (2)$$

$$E_B \equiv \frac{\hbar v_F}{l_B} \approx 26 \sqrt{B/\text{Tesla}} \text{ meV.} \quad (3)$$

Each Landau level (LL) is degenerate with density  $4\frac{e}{2\pi\hbar}B$  per unit area. Working with finite area, it is convenient to use the basis of Landau wave-functions in polar coordinates. Defining an oscillator radial eigenfunction:

$$g_{n,m}(r) = e^{-\frac{r^2}{4}} r^{|m|} \sqrt{\frac{2^{-|m|}(|m|+n)!}{2\pi n!(|m|!)^2}} {}_1F_1\left(-n; |m|+1; \frac{r^2}{2}\right)$$

we have for zeroth LL:

$$\psi_{0,m}(r, \phi) = \begin{pmatrix} 0 \\ e^{im\phi} g_{0,m}(r) \end{pmatrix}, m \leq 0 \quad (4)$$

and for  $n$ -th LL ( $m < n$ ,  $n > 0$ ):

$$\psi_{\pm n,m}(r, \phi) = \frac{e^{im\phi}}{\sqrt{2}} \begin{pmatrix} \mp e^{-i\phi} g_{n-\frac{m-1+|m|-1}{2}, m-1}(r) \\ ig_{n-\frac{m+|m|}{2}, m}(r) \end{pmatrix}$$

When the Coulomb impurity potential is present, the orbital (index  $m$ ) degeneracy of Landau levels is lifted<sup>15</sup>. This has been calculated<sup>15,19,20</sup> and demonstrated experimentally<sup>15</sup> for one Coulomb impurity. Below we consider several impurities.

Consider a superposition of Coulomb potentials of the form  $U = -\frac{e^2}{4\pi\epsilon_0\epsilon} \sum_i \frac{1}{\sqrt{(r-r_i)^2+d^2}}$ . Here the parameter  $d$  is a vertical displacement of impurity from the graphene sheet, but it can also be used to model a finite localization length of impurity wavefunction<sup>21</sup>. The equations for electron energy levels in graphene in the magnetic field  $B$  and any Coulomb potentials can be rewritten in units of magnetic length  $l_B$ , magnetic energy  $E_B$  and dimensionless coupling

$$\alpha = e^2/(4\pi\epsilon_0\hbar v_F\epsilon_{\text{eff}}) = 2.19/\epsilon_{\text{eff}} \quad (5)$$

with the effective dielectric constant  $\epsilon_{\text{eff}} = (\epsilon_1 + \epsilon_2)/2$  coming from substrates on both sides of graphene and from graphene by itself. For example,  $\alpha \approx 1$  on  $\text{SiO}_2$  substrate<sup>15</sup> and  $\alpha \approx 0.4$  on  $\text{SiC}$ . When we change the magnetic field, only  $d$  changes in the magnetic units. For small  $d$  the related change in the energy is small (not exceeds 10% when  $d$  varies in the range from 0 to  $0.1l_B$ ), so, there are almost no free parameters in the calculation. In dimensionless units the equation to solve is<sup>19</sup>

$$\begin{pmatrix} 0 & -i\partial_x - y - \partial_y \\ -i\partial_x - y + \partial_y & 0 \end{pmatrix} \Psi = \left( E + \alpha \sum_i \frac{1}{\sqrt{(r-r_i)^2+d^2}} \right) \Psi \quad (6)$$

Let us consider two positive charges. The single-particle energy levels of electron in graphene are presented on fig.2. The Landau levels that are completely filled do not contribute significantly to the energy of ions as a function of their separation: their contribution vanishes in the leading order of perturbation theory in the potential<sup>22</sup>:

$$\begin{aligned} E(r_{12}) &\sim \sum_m \langle \psi_m^{(0)} | V(\vec{r} - \vec{r}_1) + V(\vec{r} - \vec{r}_2) | \psi_m^{(0)} \rangle \\ &= 2 \sum_m \langle \psi_m^{(0)} | V(\vec{r}) | \psi_m^{(0)} \rangle = \text{const} \end{aligned} \quad (7)$$

where we used that the full (infinite) set of wavefunctions, corresponding to a given Landau level

(enumerated by  $m$ ) maps to itself under translations (up to a unitary transformation), and so the above sum is independent of the impurity positions.

The situation changes drastically if only one or several lowest Landau sub-levels are filled with electrons. This is natural when graphene is in Quantum Hall plateau state with the chemical potential somewhere in between the LLs. A landscape of such impurities is a typical microscopic picture of localized states in the description of QHE.

When the distance between the two ions is of order of magnetic length  $l_B$ , the lowest energy electron wave-function is centered between the ions and plays the role of hybridization cloud that binds them, fig. 1. When only this lowest-energy state is filled, the strong dependence of energy on the distance  $r_{12}$  between ions appears, fig. 2, creating the attractive force, fig. 3. In the leading order of perturbation theory, the binding force is proportional to  $\alpha$ . The electronic binding energy competes with Coulomb repulsion energy which reads in the magnetic units:

$$E_{Coulomb} = \frac{\alpha}{r_{12}} \quad (8)$$

Notably, it contains the same factor of  $\alpha$ , thus, in the leading approximation the distance where the attraction would balance the repulsion is independent of  $\alpha$ . We stress here that there are essentially no free parameters in the problem and the Coulomb repulsion of ions is of the same order of magnitude as hybridization attraction.<sup>23</sup> It is a-priori not at all clear if stable bound states of ions can form. Moreover, strong bound states form only when the chemical potential  $\mu$  is near the 0-th and 1-st Landau levels (when  $\mu$  is near the other Landau levels (see fig. 2), the  $r_{12}$  dependence of electron energy is substantially weaker leading to much weaker binding of ions.

For performing the computations we evaluate the matrix elements of the impurity potential in the basis (5) truncated to several Landau levels (of order of 10) and orbital states (of order of 30) and then perform an exact diagonalization. The truncation of orbital states we use corresponds to a circular box truncation of space and to avoid unphysical boundary contributions we had to smoothly cut-off the Coulomb potential at large distances (of order of  $4l_B$ ). As a result, for inter-ion distances up to  $2l_B$ , the precision is better than 1% while for larger distances the error may be higher.

First, we present the spectrum of the lowest Landau sub-levels in the field of one Coulomb impurity as a function of coupling  $\alpha$ , see Fig. 4. This will be used below to check the stability of ion bound states and shows the actual degree of non-linearity in  $\alpha$ . We see that the 0-th LL is almost protected from non-linearity, while a significant non-linearity appears in the higher LL already at  $\alpha \sim 0.1$ . As

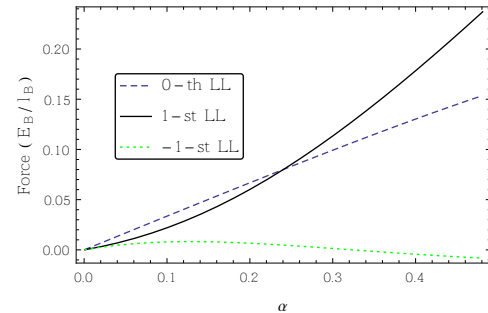


FIG. 3. Binding force of two ions bound by one electron, measured in magnetic units  $E_B/l_B$  at  $r_{12} = 1.5l_B$ .

seen on Fig. 4: The 1-st and -1-st levels must have the same energies in the leading order of perturbation theory as their wave-functions differ only by a relative sign of sublattice components, but Fig. 4 shows that these levels split already from  $\alpha \sim 0.1$ . This could be expected due to large Coulomb field near an individual impurity. For binding energy of several impurities the linearity in  $\alpha$  is better since the hybridization wave-function is mostly localized between the impurities and mixing of Landau levels is weaker, this is illustrated on fig.3 where a binding force for a typical molecule size is plotted vs  $\alpha$ . Still we observe that non-linearity near non-zero LLs is much stronger than near the 0-th LL. Below we present a particular example of  $\alpha = 0.4$ , the results are universal for 0-th LL, while for the 1-st LL the binding is seen to grow faster than linear in  $\alpha$ .

The results for two positive ions bound by one electron are presented on fig.5. We observe an absolute minimum in the energy at a distance  $r_{12\min} \approx 1.5l_B$  near the 1-st LL or  $1.7l_B$  near the 0-th LL.

If the chemical potential grows, we get more electrons to fill more levels and we have to consider multi-electron bound states. These will be discussed below. If, on the contrary, the chemical potential decreases, there will be no bound states for positive ions, but we start getting bound states for negatively charged impurities bound by holes. The calculations and results for negatively charged impurities are exactly the same and obtained by going to hole picture. The resulting schematic phase diagram is presented in table I.

Now we consider generalization of above results to binding of several positive impurities by one electron. Analogous calculation shows that the configurations with three symmetrically positioned impurities bound by one electron is unstable: despite an appearance of local minimum, the configuration would gain energy if deformed to a bound pair and repelling the third ion to infinity.

When a chemical potential is slightly higher, multi-electron bound states may form. The two-electron bound state can be in a symmetric or anti-symmetric orbital state. In a conventional molecule this would correspond to spin singlet and triplet respectively, but in graphene one has an additional

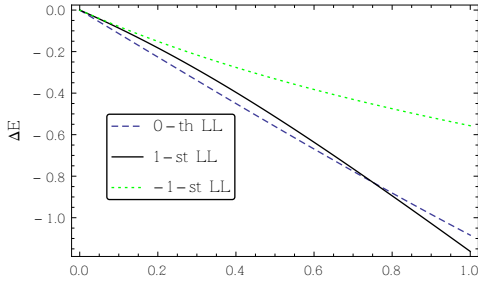


FIG. 4. Binding energy of electron in the field of one Coulomb impurity as a function of dimensionless coupling  $\alpha$ . Curves for Landau levels  $-1$ ,  $0$  and  $1$  are given, energies without impurity ( $-\sqrt{2}$ ,  $0$  and  $\sqrt{2}$ ) are subtracted.

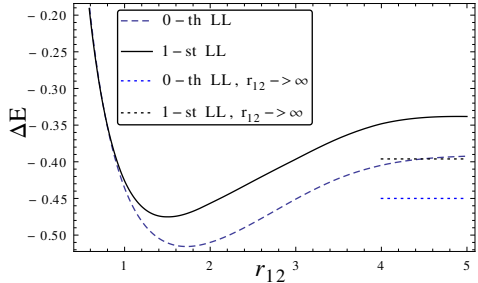


FIG. 5. Binding energy of a stable macro-molecule, consisting of two positively-charged ions bound by one electron in graphene. The two curves correspond to the filling fraction being near  $+2$  (filling of lowest sublevel of 1-st LL) or near  $-2$  (0-th LL) respectively. Here  $\alpha = 0.4$  and  $d = 0.05l_B$ . Dotted lines mark the energy of infinitely separated impurities (one is screened with an electron, another is single),

valley degeneracy<sup>24,25</sup> and the full  $SU(4)$  symmetry is approximately respected (neglecting the Zeeman splitting). Group theory tells us that  $\mathbf{4} \otimes \mathbf{4} = \mathbf{10} \oplus \mathbf{6}$  in spin-valley space, so, there are 10 possibilities to form antisymmetric orbital state and 6 for symmetric one.

To find a reasonable approximation to the energy, we use the Hartree-Fock method with the basis formed by Slater determinants of low-energy 1-particle eigenstates found above.

Looking at fig.2 we note that near the 1-st LL the two lowest energy levels grow with  $r_{12}$  thus can potentially bind the ions and can participate in antisymmetric orbital wave-function. For the 0-th LL only the lowest level binds the ions while electrons in the higher levels do not tend to hybridize, thus the orbital wave-function can only be symmetric for a stable ion-binding.

Consider two electrons in the field of a single ion. For  $\alpha = 0.4$  we have energies  $-0.28$ ,  $-0.21$  per electron in 0-th and 1-st LL respectively for symmetric state and  $-0.24$ ,  $-0.22$  respectively for antisymmetric orbital. Thus we expect symmetric state near 0-th LL and antisymmetric state near the 1-st LL. Calculation shows that one unit-charge ion can-

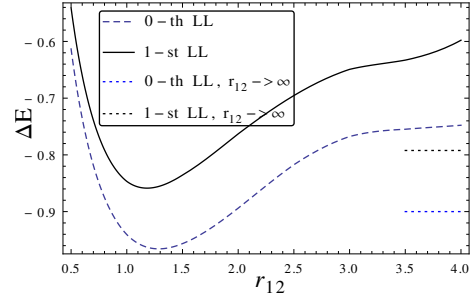


FIG. 6. Energy of a stable neutral macro-molecule, consisting of two positively-charged ions bound by two electrons in graphene,  $\alpha = 0.4$ . Symmetric state (stable). Dotted lines show the total electron energy for two far-separated impurities (taken from fig.4) thus indicating stability.

not hold more than 2 electrons in the lowest-energy states: e-e interactions make this too expensive.

Now we consider two positive charges and two electrons. Calculation shows that symmetric orbital state is preferred for two electrons near the 0-th Landau Level (LL), Fig. 6. The resulting hydrogen-like molecule is very stable with optimal inter-atomic distance  $1.2l_B$  and  $1.3l_B$  for 1-st and 0-th LL.

The same calculation can be repeated for 3 ions bound by two electrons, see fig.7. We compare the triangle configuration of ions with a linear chain geometry and find that equilateral triangle geometry has lower energy. Four ions cannot be bound by two electrons. The described equilateral triangle with 2 electrons is prominent for providing the lowest possible chemical potential for electrons, thus, it is this configuration that appears first in the phase diagram (table I).

Considering now 3-electron states in a simple Hartree approximation we found that three electrons cannot form a one-centered wave-function to bind any number of ions since the e-e interaction gets too high and the resulting energy gain can by no means compete with the energy of far-separated smaller clusters described above. Thus, with more electrons, ions will split into stable 1, 2 and 3 ion clusters described above, hence, the classification is complete. In each of the above states one can find the energy per electron in the macro-molecule cloud and thus find a minimal electron chemical potential for such molecule to appear. The calculated example phase diagram for  $\alpha = 0.4$  is presented in the table I. Changing  $\alpha$  in the leading approximation just linearly scales the phase diagram around the vacuum Landau level (0 and  $\sqrt{2}$ ).

### III. DISCUSSION AND APPLICATION

The above results were obtained for an ideal monolayer graphene sheet at zero temperature. The realistic graphene may have other non-mobile impu-

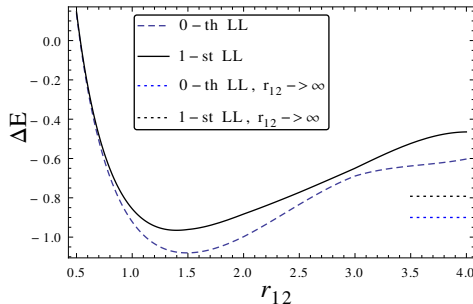


FIG. 7. Energy of three positively-charged ions in triangle geometry bound by two electrons in graphene,  $\alpha = 0.4$ , symmetric state. Dotted lines indicate the total electron binding energy for all impurities taken apart.

rities, ripples and corrugations and finite temperature. Clearly, mobile charge impurities can equally well form bound states with non-mobile ones. Simultaneously, impurities may introduce smooth inhomogeneities in the chemical potential leading to replacement of chemical potential  $\mu$  with a local chemical potential  $\mu + U_{\text{impurities}}$  in our considerations. It is also important to note that sufficient amount of mobile charged impurities leads to screening of potential landscape thus making it flat on large scales.

The effect of temperature would smear the chemical potential. As is clear from fig. 2, the binding appears when the lowest Landau sub-level is filled, while the next ones are empty. For realistic  $\alpha = 0.4$  the splitting between these levels is of the order of  $0.5E_B \approx 130\sqrt{B}/(\text{Tesla})K$  (see fig. 2). The splitting of levels is twice smaller near the 1-st LL, but in that case the second smallest LL is also attractive and it's population does not spoil the binding. So, our results must survive the room temperatures

for magnetic fields above 5 Tesla and even higher temperatures at larger fields. This opens the perspective of making ions on top of graphene mobile by increasing the temperature.

Another important aspect in graphene is rippling and corrugations<sup>26–28</sup>. As argued in ref. 29, corrugations in graphene may be described by fluctuations in perpendicular magnetic field that lead to considerable broadening of non-zero LLs. At the same time, the 0-th LL is protected and mainly broadens due to temperature. Our main results correspond to chemical potentials in the gap above or below the 0-th LL, thus the effect of corrugations is expected to be moderate. At the same time, corrugations are expected to kill any weak binding effects that might occur in the higher QHE plateaux.

To summarize, we have shown that graphene in magnetic field can mediate strong attraction of like charges put near graphene. The resulting size and configuration of macro-molecules depend on magnetic field and the number of charges and electrons (filling factor) available and thus can be easily changed by tuning magnetic field or doping of graphene. The results are expected to survive significant temperatures. This opens a thrilling perspective to nanoscopic manipulation of ions on graphene by using macroscopic tools.

*Acknowledgements:* This work has been supported by EPSRC through the grant EP/I02669X/1 and EP/H049797/1. I am indebted to Joseph J. Betouras and Feo V. Kusmartsev for stimulating discussions and support. Useful discussions with O.Gamayun and G.Berdiyorov are gratefully acknowledged.

\* S.Sлизовский@lboro.ac.uk

<sup>1</sup> K. S. Novoselov, A. K. Geim, S. V. Morozov, D. Jiang, M. I. Katsnelson, I. V. Grigorieva, S. V. Dubonos, and A. A. Firsov, *Nature (London)* **438**, 197 (2005), cond-mat/0509330.

<sup>2</sup> M. Biggs, M. Kiamahalleh, M. Mijajlovic, and M. Penna, AU2014/900273 (2014).

<sup>3</sup> M. Biggs, M. Penna, M. Kiamahalleh, and M. Mijajlovic, PCT/AU2015/000034 (2015).

<sup>4</sup> K. S. Novoselov, Z. Jiang, Y. Zhang, S. V. Morozov, H. L. Stormer, U. Zeitler, J. C. Maan, G. S. Boebinger, P. Kim, and A. K. Geim, *Science* **315**, 1379 (2007).

<sup>5</sup> H. Tetlow, J. P. de Boer, I. J. Ford, D. D. Vvedensky, J. Coraux, and L. Kantorovich, *Physics Reports* **542**, 195 (2014).

<sup>6</sup> S. Kim, J. Ihm, H. J. Choi, and Y.-W. Son, *Solid State Communications* **175** **176**, 83 (2013).

<sup>7</sup> Y. Qi, S. H. Rhim, G. F. Sun, M. Weinert, and L. Li, *Phys. Rev. Lett.* **105**, 085502 (2010).

<sup>8</sup> F. Varchon, R. Feng, J. Hass, X. Li, B. N. Nguyen,

C. Naud, P. Mallet, J.-Y. Veuillen, C. Berger, E. H. Conrad, and L. Magaud, *Phys. Rev. Lett.* **99**, 126805 (2007).

<sup>9</sup> T. J. B. M. Janssen, A. Tzalenchuk, R. Yakimova, S. Kubatkin, S. Lara-Avila, S. Kopylov, and V. I. Fal'ko, *Phys. Rev. B* **83**, 233402 (2011).

<sup>10</sup> A. Tzalenchuk, S. Lara-Avila, A. Kalaboukhov, S. Paolillo, M. Syväjärvi, R. Yakimova, O. Kazakova, T. J. B. M. Janssen, V. Fal'ko, and S. Kubatkin, *Nature Nanotechnology* **5**, 186 (2010), arXiv:0909.1220 [cond-mat.mes-hall].

<sup>11</sup> J. A. Alexander-Webber, A. M. R. Baker, T. J. B. M. Janssen, A. Tzalenchuk, S. Lara-Avila, S. Kubatkin, R. Yakimova, B. A. Piot, D. K. Maude, and R. J. Nicholas, *Phys. Rev. Lett.* **111**, 096601 (2013).

<sup>12</sup> M. M. Fogler, D. S. Novikov, and B. I. Shklovskii, *Phys. Rev. B* **76**, 233402 (2007).

<sup>13</sup> I. S. Terekhov, A. I. Milstein, V. N. Kotov, and O. P. Sushkov, *Physical Review Letters* **100**, 076803 (2008), arXiv:0708.4263.

<sup>14</sup> P. K. Pyatkovskiy and V. P. Gusynin, *Phys. Rev. B*

**83**, 075422 (2011), arXiv:1009.5980 [cond-mat.str-el].

<sup>15</sup> A. Luican-Mayer, M. Kharitonov, G. Li, C.-P. Lu, I. Skachko, A.-M. B. Gonçalves, K. Watanabe, T. Taniguchi, and E. Y. Andrei, Phys. Rev. Lett. **112**, 036804 (2014).

<sup>16</sup> Y. Zhang, Y.-W. Tan, H. L. Stormer, and P. Kim, Nature (London) **438**, 201 (2005), cond-mat/0509355.

<sup>17</sup> V. P. Gusynin and S. G. Sharapov, Phys. Rev. Lett. **95**, 146801 (2005).

<sup>18</sup> N. M. R. Peres, F. Guinea, and A. H. Castro Neto, Phys. Rev. B **73**, 125411 (2006).

<sup>19</sup> O. V. Gamayun, E. V. Gorbar, and V. P. Gusynin, Phys. Rev. B **83**, 235104 (2011).

<sup>20</sup> Y. Zhang, Y. Barlas, and K. Yang, Phys. Rev. B **85**, 165423 (2012).

<sup>21</sup> This way we may consider a hole in the “dead layer” of SiC epitaxial graphene as a mobile impurity.

<sup>22</sup> Although the Coulomb potential is large near the ion, it is the overlap of potentials of two ions that matters for the distance dependence.

<sup>23</sup> This will not be the case for the ordinary 2D electron gas since the quasiparticle mass and magnetic field will essentially enter the game.

<sup>24</sup> M. O. Goerbig, Rev. Mod. Phys. **83**, 1193 (2011).

<sup>25</sup> A. H. Castro Neto, F. Guinea, N. M. R. Peres, K. S. Novoselov, and A. K. Geim, Reviews of Modern Physics **81**, 109 (2009), arXiv:0709.1163.

<sup>26</sup> S. V. Morozov, K. S. Novoselov, M. I. Katsnelson, F. Schedin, L. A. Ponomarenko, D. Jiang, and A. K. Geim, Phys. Rev. Lett. **97**, 016801 (2006).

<sup>27</sup> J. C. Meyer, A. K. Geim, M. I. Katsnelson, K. S. Novoselov, T. J. Booth, and S. Roth, Nature (London) **446**, 60 (2007), cond-mat/0701379.

<sup>28</sup> M. I. Katsnelson and K. S. Novoselov, Solid State Communications **143**, 3 (2007), cond-mat/0703374.

<sup>29</sup> A. J. M. Giesbers, U. Zeitler, M. I. Katsnelson, L. A. Ponomarenko, T. M. Mohiuddin, and J. C. Maan, Phys. Rev. Lett. **99**, 206803 (2007).